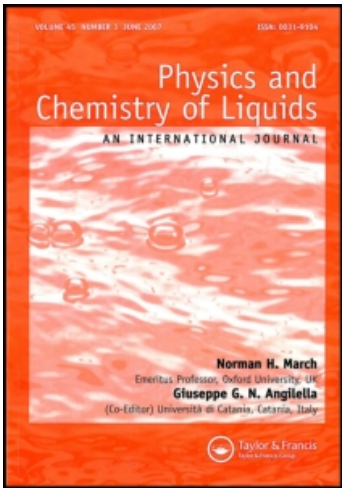

Physics and Chemistry of Liquids
Publication details, including instructions for authors and subscription information:
http://www.informaworld.com/smpp/title~content=t713646857

Evidence of Chemical Short Range Order in Molten CuTi Alloys

He. Fenglai[ab]; N. Cowlam[a]; G. E. Carr[ac]; J. B. Suck[d]
[a] Department of Physics, University of Sheffield, Sheffield, UK [b] Department of Basic Science, Shanghai Building Material Institute, Jiangwan, Shanghai, Peoples Republic of China [c] Department of Metallurgy, Univerity of Sheffield, Sheffield, UK [d] Kernforschungszentrum Karlsruhe, Institut für Nukleare Festkörperphysik, Karlsruhe, FRG

To cite this Article Fenglai, He. , Cowlam, N. , Carr, G. E. and Suck, J. B.(1986) 'Evidence of Chemical Short Range Order in Molten CuTi Alloys', Physics and Chemistry of Liquids, 16: 2, 99 — 112
To link to this Article: DOI: 10.1080/00319108608078506
URL: http://dx.doi.org/10.1080/00319108608078506

Phys. Chem. Liq., 1986, Vol. 16, pp. 99–112
0031-9104/86/1602-0099$18.50/0

Printed in the United Kingdom

Evidence of Chemical Short Range Order in Molten CuTi Alloys

HE. FENGLAI,† N. COWLAM, G. E. CARR‡

Department of Physics, University of Sheffield, Sheffield S3 7RH, UK.

and

J.-B. SUCK

Kernforschungszentrum Karlsruhe, Institut für Nukleare Festkörperphysik, POB 3640, D7500 Karlsruhe, FRG.

(*Received March 25, 1986*)

Neutron diffraction measurements have been made on a series of four CuTi molten alloy samples in order to determine the possible variation of chemical short range order (CSRO) with composition in the liquid state. The structure factor curves $S(Q)$ obtained all contain the characteristic pre-peak at $Q \sim 1.9$ Å^{-1} which provides experimental evidence for the existence of CSRO. The degree of CSRO present has been estimated and the CSRO parameter α obtained from an analysis based on experimental and calculated $S(Q)$ curves. The observed variation of CSRO with composition in the liquid state follows the trends established from previous experiments and thermodynamic calculations. The CSRO is less developed in the melt than in the metallic glass phase.

1 INTRODUCTION

Chemical short range order (CSRO) is known to exist between the constituents in certain metallic alloy glasses[1,2] and has been shown to be a possible factor which influences the stability of the glassy phase. Diffraction measurements on CuTi metallic glasses have demonstrated a direct correlation between the Cowley[3] CSRO parameter α and the crystallisation temperature

† Permanent address: Department of Basic Science, Shanghai Building Material Institute, No 100 Wudong Road, Jiangwan, Shanghai, Peoples Republic of China.

‡ Present address: Department of Metallurgy, Univerity of Sheffield, Sheffield S1 3JD, UK.

of the glass, over an extended composition range.[4] The observed variation of α with composition has been shown subsequently to be in good overall agreement with the results of thermodynamic calculations on molten CuTi alloys.[5,6]

It is necessary to determine the origin of this CSRO in order to establish its importance in relation to other mechanisms which have been proposed to account for the stability of metallic glasses. The process of melt-spinning used to produce metallic glass specimens and the fact that eutectic minima in the alloy phase diagrams can be important indicators of good glass-forming ability[7] suggest intuitively that CSRO in the glass must originate in the molten state. However, whilst eutectic minima may imply strong interatomic correlations in the melt, diffraction experiments are, in general, better at providing information about topological correlations (TSRO) rather than the chemical correlations (CSRO) which may be involved.

The studies on CuTi[1] and NiTi[2] glasses referred to above exploit the resonant, as opposed to potential, scattering of neutrons from titanium nuclei, described by a negative value of scattering amplitude $b_{Ti} = -0.3438 \times 10^{-12}$ cm. This "negative" scattering enhances the contrast between the alloy species and gives an unsurpassed sensitivity to chemical ordering effects in the neutron experiments. Figuratively, the copper and titanium nuclei appear as black and white scattering centers to neutrons rather than their electron clouds appearing as different shades of grey as with an X-ray beam. We have exploited this effect in a preliminary measurement of CSRO in a liquid $Cu_{66}Ti_{34}$ alloy,[8] the results of which show that the CSRO does indeed exist in the liquid state as well as in the glass. In this present study new measurements are presented on four molten CuTi alloys which demonstrate that the CSRO in the melt follows the same trend with composition as established so far, both by experiments on the glasses[4] and from thermodynamic calculations.[5,6]

2 EXPERIMENTAL METHOD AND DATA ANALYSIS

2.1 Experimental considerations

Ideally it would be valuable to measure the variation of CSRO in molten CuTi alloys across at least the glass forming, if not the entire composition range. However for several practical reasons, the present measurements extend from 80% copper to 57% copper and include approximately half the glass forming range. The reasons for this are threefold.

First is the question of the possible *extent* of the CSRO. Strongly negative values of the enthalpy of mixing ΔH are usually accepted as being indicative

of heterogenous atomic arrangements and specifically a strong attractive interaction between unlike atoms. The measured values of ΔH for molten Cu_xTi_{1-x} alloys have a strong compositional dependence—like $x(1-x)$, with the lowest values $-\Delta H \sim 3$ kJ/mol in the *equiatomic* region.[5,9]

Next is the question of the *visibility* of the CSRO in a diffraction experiment. The natural framework for this is the formulation of the total structure factor $S(Q)$ of Bhatia and Thornton.[10]

$$S(Q) = \frac{\langle b\rangle^2 S_{NN}(Q) + 2\langle b\rangle \Delta b S_{NC}(Q) + \Delta b^2 S_{CC}(Q)}{\langle b^2\rangle} \tag{1}$$

Here b is the scattering amplitude

$$\langle b\rangle = x b_{Cu} + (1-x) b_{Ti}$$
$$\langle b^2\rangle = x b_{Cu}^2 + (1-x) b_{Ti}^2$$
$$\Delta b = b_{Cu} - b_{Ti}$$

$S_{NN}(Q)$ relates to density (TSRO) variations. Its Fourier transform gives the Radial Distribution Function RDF $= 4\pi r^2 \rho_{NN}(r)$ from which the coordination number $\langle n\rangle$ is obtained. $S_{CC}(Q)$ relates to compositional variations. Its Fourier transform gives the radial concentration function RCF $= 4\pi r^2 \rho_{CC}(r)$ from which the Cowley[3] CSRO parameter α is obtained. $S_{NC}(Q)$ is a "size effect" cross term (which can be neglected in a first approximation if the size difference between the species is not excessive).[2] The coefficients for $S_{NN}(Q)$ and $S_{CC}(Q)/x(1-x)$ can be written for a binary alloy as $\omega_{NN} = \langle b\rangle^2/\langle b^2\rangle$ and $\omega_{CC} = 1 - \omega_{NN}$ respectively, see Table I. Thus if $S_{NC}(Q)$ is negligible this gives an obvious division of the total $S(Q)$ into TSRO and CSRO components.

$$S(Q) \approx \omega_{NN} S_{NN}(Q) + \omega_{CC} S_{CC}(Q)/x(1-x) \tag{2}$$

If, as here, one component of the alloy has a negative value of scattering length, then the relative concentration of the constituents can be chosen so that $\langle b\rangle$ and ω_{NN} are zero at the "null matrix" alloy, scattering from which relates to CSRO alone. This occurs for an alloy composition close to $Cu_{31}Ti_{69}$ so therefore CSRO is *most visible in titanium rich* alloys.

Finally, there is the experimental accessibility of the specimens, which depends on both their melting point and the containment of the molten alloys. The lowest melting points ~ 860°C occur for alloys around the shallow eutectic at $Cu_{73}Ti_{27}$. Even at these relatively low temperatures the reactivity of these titanium-based samples is a severe problem. The container must not only remain intact for the (significant) period of the neutron experiment but must also have suitable transmission and scattering characteristics in the neutron beam. Trials with conventional materials such as quartz, graphite and refractories showed that stainless steel provided the

TABLE I

The weighting factors for the Bhatia-Thornton and Faber-Ziman partial structure factors (PSF's) are given for the four molten alloys examined. The observed and calculated first neighbour distances r_1 of the RDF are given and the estimated values of coordination number $\langle n \rangle$ and CSRO parameter α.

Alloy Composition	Weighting factors for PSF's					First neighbour distance (Å)			Coord. No. $\langle n \rangle$ ± 0.3	CSRO parameter α ± 0.01
	Bhatia-Thornton		Faber-Ziman							
	ω_{NN}	ω_{CC}	ω_{CuCu}	ω_{CuTi}	ω_{TiTi}	r_1^{obs}	r_1^{G}	r_1^{FZ}		
$Cu_{80}Ti_{20}$	0.602	0.398	1.266	−0.282	0.016	2.53	2.64	2.51	11.9	−0.03
$Cu_{73}Ti_{27}$	0.474	0.526	1.433	−0.472	0.039	2.51	2.66	2.49	11.7	−0.06
$Cu_{66}Ti_{34}$	0.356	0.644	1.684	−0.773	0.089	2.50	2.69	2.45	11.5	−0.08
$Cu_{57}Ti_{43}$	0.219	0.781	2.268	−1.525	0.256	2.46	2.72	2.37	11.2	−0.07

most appropriate choice of container. However, even with this material, experiments were limited to *copper rich alloys* whose reactivity was smallest.

2.2 Method and data analysis

Master ingots in the shape of rough cylinders were made of four alloys $Cu_{80}Ti_{20}$, $Cu_{73}Ti_{27}$, $Cu_{66}Ti_{34}$ and $Cu_{57}Ti_{43}$, by argon arc melting spectroscopically pure materials and casting on a copper hearth. These ingots were machined to fit the thin-walled stainless steel containers used, which had an inner diameter of 6 mm.

A series of neutron measurements was made using the D4B diffractometer with an incident wavelength of $\lambda = 0.7$ Å, at Institute Laue Langevin, Grenoble. The $Cu_{80}Ti_{20}$, $Cu_{73}Ti_{27}$, $Cu_{66}Ti_{34}$ and $Cu_{57}Ti_{43}$ samples were examined at temperatures of 1000 °C, 910 °C, 950 °C and 1010 °C respectively. A thin-walled vanadium furnace element was used in the conventional evacuated bell jar. A wide range of scattering angles $1.9° < 2\theta < 69.3°$ in 0.1° steps, and $49.8° < 2\theta < 133.6°$ ($Q_{max} = 16.5$ Å^{-1}) in 0.2° steps was covered by the two multi-anode detectors. Experimental times from five hours down to two hours for the most reactive specimen ($Cu_{57}Ti_{43}$), were used. Sample container scans were also made at four temperatures to expedite the background subtraction which had a high component of Bragg peaks. Empty furnace, vanadium standard and cadmium background scans were also made within a four day experimental period.

The data were analysed and corrected using our own programs covering the scattering from the empty containers and furnace, absorption and multiple scattering of neutrons in the sample and the Placzek correction of the sample scattering. Normalisation was made with reference to both the vanadium standard and the self-normalisation method.[11]

The total structure factors $S(Q)$ (Eqs 1 and 2) for the four specimens are shown in Figure 1. The statistical quality of the raw data was extremely good so that notwithstanding the high component of Bragg peaks in the background subtraction, the $S(Q)$ are very well defined and a fifth oscillation in $S(Q)$ at $Q \sim 14$ Å^{-1} is visible in the Figure. The four $S(Q)$ curves show a gradual evolution in form as the contributions from $S_{NN}(Q)$ and $S_{CC}(Q)$ change according to the weighting factors in Table I. However, all the curves have the same general characteristics as those of the metallic glasses[4] and the single molten alloy studied previously,[8] namely a pre-peak between $1.8 < Q < 1.9$ Å^{-1} and the first true or main peak at $3.0 < Q < 3.1$ Å^{-1}. It is noticeable that there is also some broadening of the peak at $Q \sim 5.5$ Å^{-1} for the $Cu_{66}Ti_{34}$ and $Cu_{57}Ti_{43}$ specimens of the kind normally associated with the glassy state—although of course these samples were melted directly from crystalline ingots. The presence of the pre-peak is itself a valuable indication

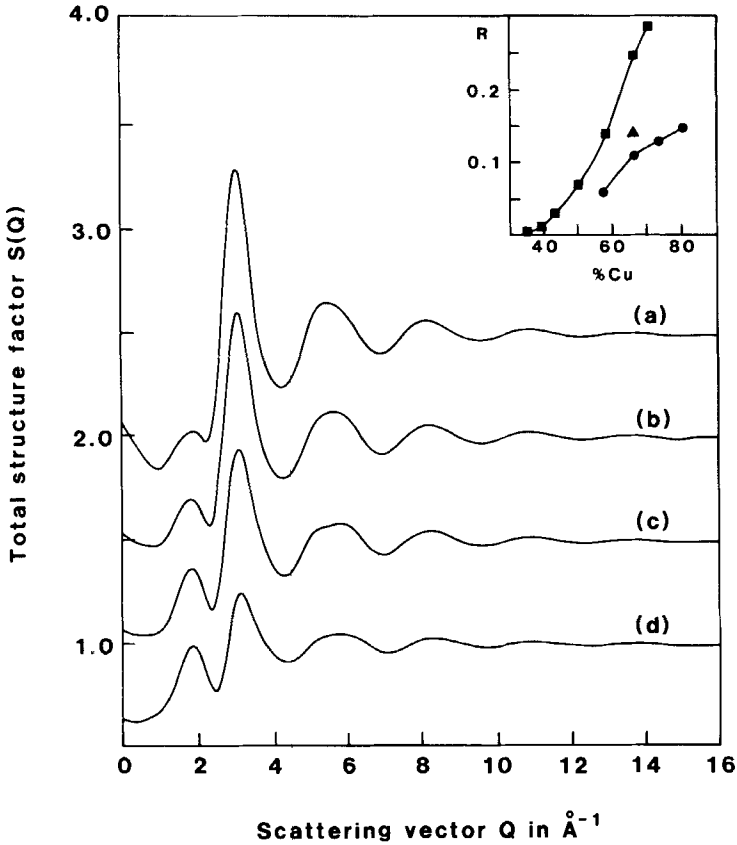

FIGURE 1 The total structure factors for four CuTi molten alloys (a) $Cu_{80}Ti_{20}$, (b) $Cu_{73}Ti_{27}$, (c) $Cu_{66}Ti_{34}$ and (d) $Cu_{57}Ti_{43}$ are shown. In the insert the variation of the ratio R, given in the text, with composition is shown. Molten alloys ● present and ▲ previous work,[8] ■ glassy alloys.[4]

of CSRO and the alloy systems for which $S(Q)$ exhibits such a feature have been enumerated.[2] However, neither the absolute nor the relative magnitude of the pre-peak can be taken as a measure of this CSRO for a series of total $S(Q)$ curves, as here, since the relative contributions of $S_{NN}(Q)$ and $S_{CC}(Q)$ vary as a function of composition according to ω_{NN} and ω_{CC}. Thus instead of using the peak heights, the normalised ratio $R = (S_p(Q)/\omega_{CC} - 1)/(S_1(Q)/\omega_{NN} - 1)$ where $S_p(Q)$ and $S_1(Q)$ are the values of $S(Q)$ at the pre-peak and first-peak respectively, can form a more realistic measure of the likely CSRO in the sample. The value of this ratio is plotted in the insert to Figure 1, which shows that it follows the same general trend with composition in both the liquid and glassy states.

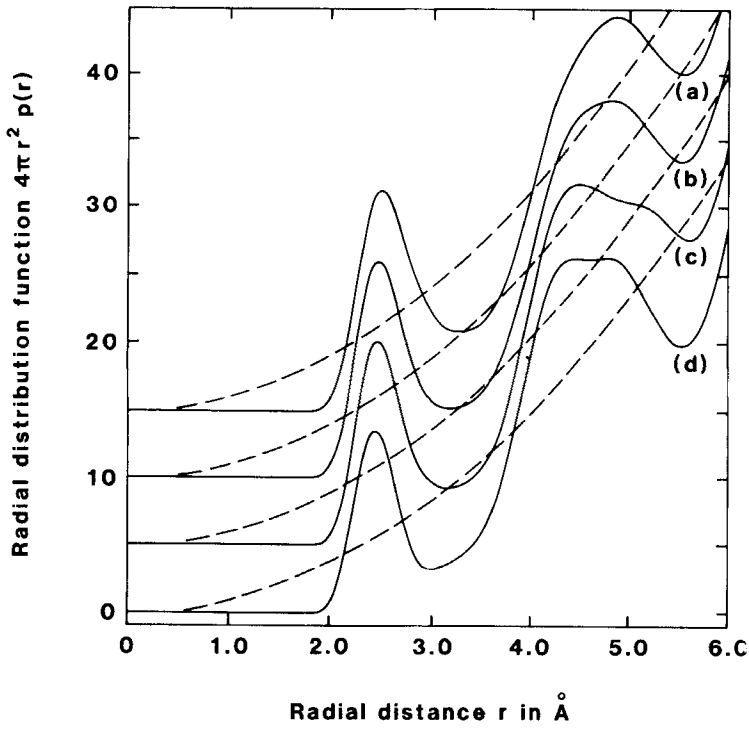

FIGURE 2 The Radial Distribution Functions resulting from the Fourier Transforms of the total $S(Q)$ curves given in Figure 1 are shown, with the same identification (a) to (d).

The total RDF's for the four specimens are shown in Figure 2 and have the conventional form. The absence of spurious ripples at small radial distances in the RDF (and associated curves) illustrates that the normalisation of $S(Q)$ is substantially correct. Some care has to be taken in the determination of the first neighbour distance r_1 and the coordination number $\langle n \rangle$ from these total RDF's.

As an illustration of this, the position of the first peak recorded in the RDF's r_1^{obs} appears to decrease with increasing titanium concentration, Table I. Titanium is the larger atom and values based on the Goldschmidt diameters of the constituents r_1^G therefore increase with titanium content. This anomaly can be understood most clearly in terms of the alternative Faber-Ziman[12] partial structure factors

$$S(Q) = \frac{x^2 b_{Cu}^2 S_{CuCu}(Q) + 2x(1-x) b_{Cu} b_{Ti} S_{CuTi}(Q) + (1-x)^2 b_{Ti}^2 S_{TiTi}(Q)}{\langle b \rangle^2} \quad (3)$$

$$S(Q) = \omega_{CuCu} S_{CuCu}(Q) + \omega_{CuTi} S_{CuTi}(Q) + \omega_{TiTi} S_{TiTi}(Q) \quad (4)$$

Both the partial structure factor $S_{CuTi}(Q)$ and the partial atomic density $\rho_{CuTi}(r)$ have *negative* coefficients ω_{CuTi}, see Table I, which perturb the way in which the total $S(Q)$ and total RDF are usually constructed. Thus a weighted average of Cu-Cu, Cu-Ti and Ti-Ti first neighbour distances r_1^{FZ} based on the Faber-Ziman coefficients above, decreases with titanium concentration in agreement with observation (see Table I).

3 AN ESTIMATE OF THE EXTENT OF THE CHEMICAL SHORT RANGE ORDER

It seemed worthwhile to obtain some measure of the variation of the CSRO with composition for these alloys in view of the paucity of data in this area and the potential usefulness of the results. However, it is important to stress that an *exact* result as from the partial structure factors can *never* be obtained from a single experiment although, as will be shown below, some measure of consistency can be achieved even in an approximate analysis.

The degree of approximation involved can be considered at two levels. First is the question of the size difference of the species—whether the term $S_{NC}(Q)$ can be neglected, that is whether Eq. (1) or (2) above should be used. In several examples in the past it has been possible to neglect the $S_{NC}(Q)$ contribution to $S(Q)$ and the circumstances under which this can be done have been discussed.[2] We have established in analysis of structure factors for CuTi glasses,[13] that using a model for $S_{NC}(Q)$, rather than neglecting the term entirely, does not significantly alter the values of CSRO parameter obtained.

Thus if we choose to neglect $S_{NC}(Q)$ in the present analysis, so that $S(Q)$ can be approximated to a weighted sum of $S_{NN}(Q)$ and $S_{CC}(Q)$ terms alone (Eq. 2), then the CSRO parameter α can be obtained from the Fourier transform of $S_{CC}(Q)$. A possible source of the $S_{NN}(Q)$ curves is from X-ray experiments, in which case a simultaneous solution for $S_{NN}(Q)$ and $S_{CC}(Q)$ can be made from neutron and X-ray data together[2,4] and this clearly involves no further approximation. However, there are at present no X-ray data available, as far as we are aware, on liquid CuTi alloys. In our previous investigation of the molten $Cu_{66}Ti_{34}$ alloy[8] the experimental structure factor for liquid copper[14] was used to imitate $S_{NN}(Q)$ in order to obtain an estimate of α. Since that time we have used a simple hard sphere model[15] for $S_{NN}(Q)$ with some success in the analysis of metallic glass data.[16] These curves also represent a valid choice for liquid metal alloys and so have been used in the present estimates.

The analysis was made as follows. A calculated $S_{NN}(Q)$ curve was produced and the product $\omega_{NN}S_{NN}(Q)$ subtracted from the total $S(Q)$. The curve $S_{CC}(Q)$ was deduced from the remainder and Fourier transforms were made of both $S_{NN}(Q)$ and $S_{CC}(Q)$ curves and these were examined. The form of the calculated $S_{NN}(Q)$ depended on the choice of hard sphere diameter σ and

packing fraction η,[15] which determined the positions and amplitudes of the peaks in $S_{NN}(Q)$ respectively. The procedure described above, starting from the production of the $S_{NN}(Q)$ through to the Fourier transforms, RDF and RCF was repeated for several choices of σ around 2.3 Å and η around 0.50. The following factors acted as checks on whether an appropriate choice had been made. First the $S_{CC}(Q)$ curve derived had to oscillate about the limiting value $x((1-x)$ and this was influenced by the amplitude of $S_{NN}(Q)$ and the choice of η. Second the Fourier Transform of $S_{CC}(Q)$ (the RCF) can only differ from zero at proper radial distances corresponding to features in the RDF. This self-consistency check is frequently used for crystalline materials having CSRO[17] but it is also generally true of disordered and liquid structures. Finally, both the Fourier transforms of $S_{NN}(Q)$ and $S_{CC}(Q)$ had to contain the minimum of spurious ripple—whose effect can be monitored in forward and back transforms.

This approximate procedure was clearly most successful for the alloys with the highest titanium concentrations for which $S(Q)$ is already dominated by $S_{CC}(Q)$ (see Table I). Figure 3 shows the total $S(Q)$ for the $Cu_{66}Ti_{34}$ alloy and

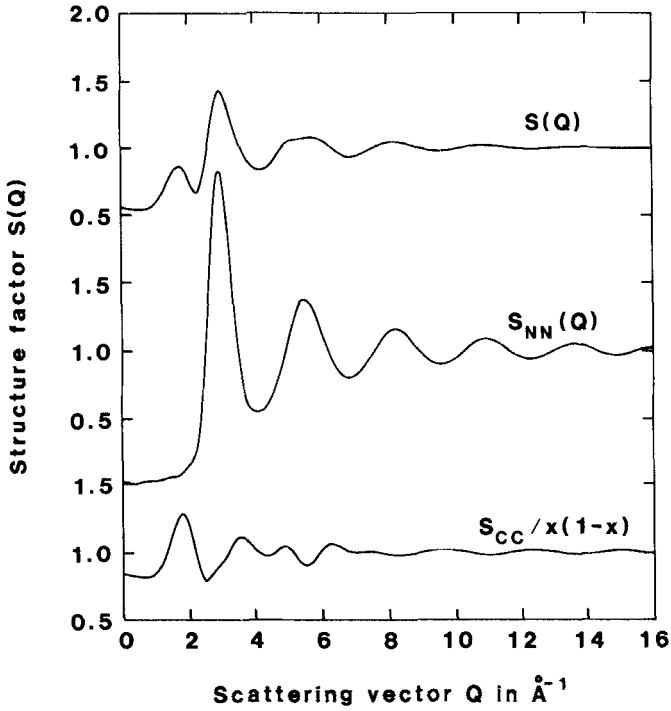

FIGURE 3 The subdivision of the total structure factor $S(Q)$ into $S_{NN}(Q)$ and $S_{CC}(Q)/x(1-x)$ components, according to Eq. (2) in the text, is shown for the $Cu_{66}Ti_{34}$ molten alloy.

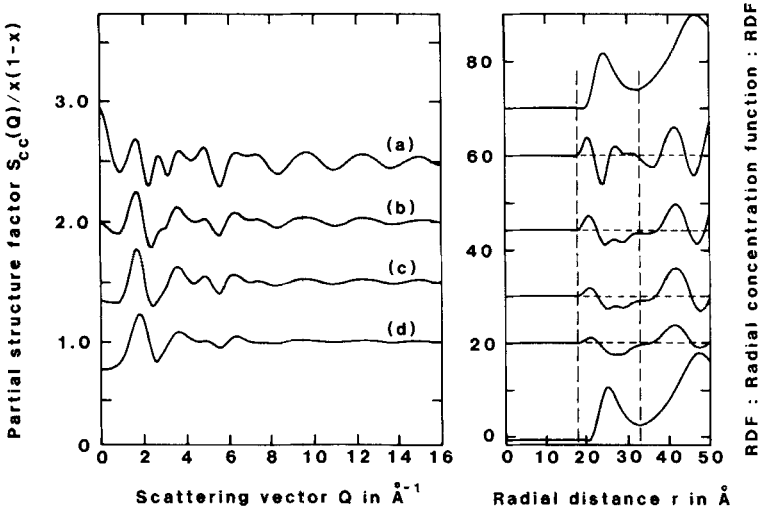

FIGURE 4 The curves $S_{CC}(Q)/x(1-x)$ derived for the (a) $Cu_{80}Ti_{20}$, (b) $Cu_{73}Ti_{27}$, (c) $Cu_{66}Ti_{34}$ and (d) $Cu_{57}Ti_{43}$ molten alloys are shown in the left hand side of the figure. In the right hand side the four central graphs show part of the RCF's derived from the Fourier transform of these $S_{CC}(Q)$ curves. The upper and lower curves give the RDF's for $Cu_{80}Ti_{20}$ and $Cu_{57}Ti_{43}$ respectively and the vertical lines define the radial limits of the first neighbour peak.

the two curves $S_{NN}(Q)$ and $S_{CC}(Q)$ into which it is decomposed according to Eq. 2. Figure 4 shows the $S_{CC}(Q)$ curves obtained for all four CuTi samples and each exhibits a first peak which coincides in position with the pre-peak in the total $S(Q)$. The $S_{CC}(Q)$ curve for $Cu_{80}Ti_{20}$ is least well defined (this alloy has the smallest value of the coefficient ω_{CC}) and the detailed oscillations beyond the first peak are probably spurious. The Radial Concentration Function RCF $= 4\pi r^2 \rho_{CC}(r)$ curves are also shown in Figure 4. The RCF curves oscillate about zero depending on whether like (+ve) or unlike (−ve) atomic correlations occur. The integrated area of the RCF over the values of radial distance which define the first neighbour peak, shown dotted in the figure, is equal to the product $\langle n \rangle \alpha$. Once again the curve for the $Cu_{80}Ti_{20}$ alloy shows the most uncertainty, but for each higher titanium concentration the curve has a clear negative region around 2.6 Å, indicative of unlike atomic correlations (−ve/negative) at the first neighbour distance. Incidentally, the curves also have a positive region at $r \sim 4.2$ Å showing longer range like-atom correlations from which the pre-peak originates through the relation[18] $r_p = \frac{5}{4}\, 2\pi/Q_p$ where $Q_p \sim 1.9$ Å^{-1}. The *estimated* values of the CSRO parameter α and coordination number $\langle n \rangle$ for the four alloys are given in Table I. The coordination number depends on the value of packing fraction and the mean density ρ_0. The values obtained are close to the experimental value of $\langle n \rangle = 11.5$ for liquid copper.[14] The hard-sphere

diameter σ does not, however, coincide perfectly with the real values of interatomic distance as is often found to be the case in this kind of simulation.[16] The errors in the values of α and $\langle n \rangle$ given in Table I have been estimated with regard to the possible range of choice of σ and η in analysis described above.

4 DISCUSSION AND CONCLUSIONS

The values of the Cowley CSRO parameter α estimated in the present analysis are shown in Figure 5 together with the corresponding values obtained for CuTi metallic glasses[4] and the single value from the preliminary measurement on liquid $Cu_{66}Ti_{34}$.[8] The solid lines in the figure represent the calculated variation with composition of the "mole number of $n_{Cu_3Ti_2}$ associates" as defined and calculated by Sommer *et al.*[5] for sample temperatures of 700 K (supercooled liquid) and 1173 K (molten state). Even though it is not possible to make a too detailed interpretation of this figure in view of

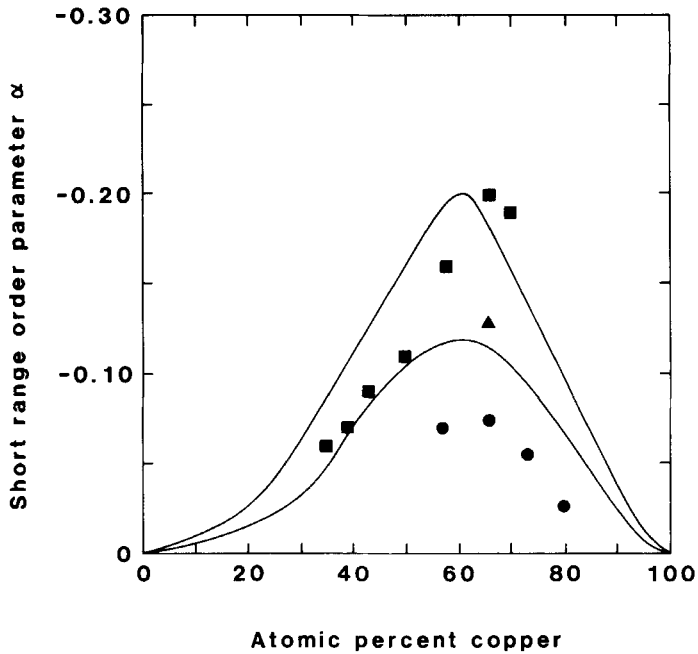

FIGURE 5 The variation of the Cowley short range order parameter α with composition is shown. Molten alloys—values estimated from ● the present and ▲ the previous[8] analyses, ■ glassy alloys.[4] The solid lines represent the variation with composition of the "mole number of $n_{Cu_3Ti_2}$ associates" for temperatures of $T = 1173$ K lower curve and $T = 700$ K upper curve respectively.[5]

the approximate methods used in the analysis above. However, two general points appear to be valid.

First, the CSRO in both liquid and glassy states appears to follow a regular variation with composition, probably peaking around the 66:34 or equi-atomic concentrations. The CSRO is true short-range order (α values negative) for all compositions unlike, say, Cu-Mn liquid alloys for which both short range order and clustering may occur at different alloy concentrations.[19] This behaviour may help to account for the extended glass-forming range of the CuTi alloys.[4]

Second, the CSRO is obviously less well developed in the melt than in the glass and this is consistent with the theoretical prediction (Ref. 5 and S. J. Gurman—private communication). This result originates in the measurements of peak height—the ratio R, plotted in Figure 1 and is confirmed by the approximate analysis made in Section 3. It seems unlikely that this analysis, say, for the molten $Cu_{57}Ti_{43}$ sample, could be significantly altered even by quite drastic changes in the $S_{NN}(Q)$ chosen, which makes only a minor contribution to the total $S(Q)$. Equally, the omission of $S_{NC}(Q)$ becomes less significant for these small values of α.[2]

Figure 5 appears to show that there may be an increase of the order of 100% in the value of α on vitrification, although it may be unwise to place too much weight on the precise *numerical* relationship in view of the approximate analysis performed above. This is also borne out by the relatively poor agreement between the two values of α for the $Cu_{66}Ti_{34}$ composition, in the present work and previous study.[8] Incidentally, this disagreement probably arises from two factors, first that the data were recorded at different temperatures 950°C and 875°C[8] respectively. Second, it was possible to perform the normalisation of the total $S(Q)$ more rigorously in the present work than in the preliminary experiment.[8] Different curves for $S_{NN}(Q)$ where incidentally used in the two cases.

Finally, it is interesting to consider possible mechanisms by which the CSRO in the melt can be enhanced on vitrification. Chemical rearrangements in the local atomic groupings may occur which minimise the total energy, possibly by means of thermally activated diffusion. A value of $\alpha = -0.1$ for the liquid state represents about 0.8 atom of the first neighbour shell of 12 being 'misplaced' from the random configuration and $\alpha = 0.20$ about 1.6 atoms displaced from random in the glassy state.[4] An absolute *minimum* number of favourable jumps per atom $n_j = 0.8/12 = 0.067$ are therefore needed to produce the observed change in α at vitrification. There are three stages in the melt spinning process where these changes may occur and the expression for the jump frequency ν_j

$$\nu_j = \nu_D \exp(-E/kT) \tag{5}$$

can be used with parameters from these stages to assess the likelihood of this happening. The initial vitrification takes place on the cold rotating drum at an undercooled temperature of around 60% of the melting temperature, i.e. $T_1 \approx 0.6 \times 1250 \approx 750$ K for CuTi glasses. This is followed by a post quench anneal of the still-hot ribbon to which we have drawn attention previously.[20,21] Two stages can be identified in this, a short period when the ribbon remains in contact with the drum, say $T_2 \sim 550$ K and finally, a longer period of free flight through the air or inert atmosphere surrounding the equipment, say $T_3 \sim 400$ K. Characteristic times within which the diffusion jumps must occur can be identified with these three stages. A typical quenching rate for melt-spinning is 10^6 K s^{-1}, so arbitrarily $t_1 \sim 10^{-6}$ s, while for a drum (rim) speed of 20 m s^{-1} and a 0.05 m contact length one finds $t_2 = 2.5 \times 10^{-3}$ s, and a 2.0 m flight of the ribbon gives $t_3 = 0.1$ s. Substituting these three times and temperatures, together with the assumed $n_j = 0.067$ and $\nu_D = 10^{12}$ Hz into Eq. 5 yields values of activation energy for diffusion E between 0.9–1.1 eV (gratifyingly close to the measured values for metallic glasses[22]) for the three stages of the process. Thus the increase in CSRO parameter on vitrification is consistent with thermally activated diffusion occurring during the process, although it must be said that the exponential in Eq. 5 means that ν_j can be changed by one or even two orders of magnitude without too drastic results on the value of E obtained.

More generally, the subject of chemical ordering in liquid metal alloys seems worthy of further investigation both for its own sake and in relation to its possible influence on glass formation. We are currently extending these measurements to other binary alloy systems which allow a full derivation of the three partial structure factors to be made without further approximations.

Acknowledgements

This work has been supported by the Science and Engineering Research Council. The neutron diffraction measurements were made at the Institute Laue Langevin, Grenoble. The authors are pleased to acknowledge the help received from Dr. P. Chieux, Dr. R. Meyer and Mr. A. Hawes. Dr. S. J. Gurman has also provided details of his most recent work on molten transition metal alloys.

References

1. M. Sakata, N. Cowlam and H. A. Davies, *J. Phys. F: Metal Phys.*, **9**, L235–40, 1979.
2. H. Ruppersberg, D. Lee and C. N. J. Wagner, *J. Phys. F: Metal. Phys.*, **10**, 1645–52, 1980.
3. J. M. Cowley, *Phys. Rev.*, **77**, 667–675, 1950.
4. M. Sakata, N. Cowlam and H. A. Davies, Proc. 4th Int. Conf. Rap. Quench. Met., **1**, 327–30, 1982 (Jap. Inst. Met: Sendai).
5. F. Sommer, K.-H. Klappert, I. Arpshofen and B. Predel, *Z. Metallk*, **73**, 581–4, 1982.
6. S. J. Gurman, Solid State Physics Conference, Institute of Physics, Southampton 1984 (Abstract).

7. H. A. Davies, *Phys. Chem. Glasses*, **17**, 159-173, 1976.
8. M. Sakata, N. Cowlam and H. A. Davies, *J. Phys. F: Metal. Phys.*, **11**, L157-62, 1981.
9. H. Yokokawa and D. J. Kleppa, *J. Chem. Thermodynam*, **13**, 703-15, 1981.
10. A. B. Bhatia and D. E. Thornton, *Phys. Rev., B.*, **2**, 3004-12, 1970.
11. J. E. Enderby in *Physics of Simple Liquids*, ed. H. N. V. Temperley, J. S. Rowlinson and G. S. Rushbrooke, Amsterdam: North Holland, pp. 613-43.
12. T. E. Faber and J. M. Ziman, *Phil. Mag.*, **11**, 153-73, 1965.
13. N. Cowlam, He. Fenglai, P. P. Gardner, M. Sakata and H. A. Davies (to be published).
14. C. N. J. Wagner, H. Ocken and M. L. Joshi, *Z. Naturforsch*, **20a**, 325-35, 1965.
15. N. W. Ashcroft and J. Lekner, *Phys. Rev.*, **145**, 83-90, 1966.
16. Wu. Guoan, N. Cowlam and M. R. J. Gibbs, *J. Mat. Sci.*, **19**, 1374-84, 1984.
17. B. E. Warren, X-ray diffraction (Addison-Wesley: Reading Mass) pp. 232.
18. H. P. Klug and L. E. Alexander, X-ray diffraction procedures, John Wiley, New York, 847-9, 1974.
19. S. Sato and O. J. Kleppa, *Metall Trans.*, **10B**, 63-6, 1979.
20. K. Dini, N. Cowlam and H. A. Davies, *J. Phys. F: Metal. Phys.*, **12**, 1553-66, 1982.
21. N. Cowlam, K. Dini, P. P. Gardner and H. A. Davies, *J. Phys. Chem. Liq.* **15**, 253-64, 1986.
22. M. Kijek, D. Akhtar, B. Cantor and R. W. Cahn, Proc. 4th Int. Conf. Rap. Quen. Met., **1**, 573-7, 1982 (Jap. Inst. Met.: Sendai).